



Spatial variations in physico-chemical characteristics of PM_{2.5} in an urban coastal city of India and associated health risks

Shruti Tripathi¹ · Abhishek Chakraborty¹ · Debayan Mandal¹

Received: 2 February 2023 / Accepted: 6 June 2023 / Published online: 3 July 2023
© The Author(s), under exclusive licence to Springer Nature B.V. 2023

Abstract

This paper investigates the chemical composition of Particulate Matter, Organic Carbon (OC), and Elemental Carbon (EC) in residential and traffic sites in Mumbai. The average PM_{2.5} and PM₁₀ concentrations at the traffic site (Sakinaka) were 240 µg/m³ and 424 µg/m³, respectively. The observed levels of OC were 35 µg/m³, 22 µg/m³, and 15.5 µg/m³ at Sakinaka junction (high-density traffic), YP-Gate (low-density traffic), and Hostel Premise (Residential), respectively. The average OC/EC ratio value was high (4.5) at the residential site, indicating contributions from stationary combustion sources and secondary production of carbonaceous species to OC. The residential site has a higher percentage of low volatile OC fraction (57%) in total OC than the traffic sites. On the other hand, Sakinaka has a higher percentage of highly volatile OC fractions (36%) in total OC. The crustal-originated metals were dominating in all areas, but the concentration of metals from anthropogenic sources was highest at Sakinaka, i.e., As (381 ng/m³), Pb (352 ng/m³), Zn (679 ng/m³). The K/Al, Ca/Al, Mg/Al, and Fe/Al ratios were high in all the samples compared to the crustal ratio indicating biomass burning and traffic emission sources of these metals. PM originating from traffic was more enriched with heavy metals that are toxic to human health, increasing cancer risks (CR) through inhalation. The hazard quotient was above 1 at all the locations, and CR was above 1 × 10⁻⁴, causing health risks. According to the dosimetry model, more PM was deposited in the lungs of traffic location occupants through inhalation, increasing the cancerous risk.

Keywords Organic Carbon · Elemental Carbon · Organic Aerosol · Char-EC and Soot-EC · Risk assessment · Lung deposition

1 Introduction

Air pollution is the leading cause of worldwide premature death. Around 7 million people die prematurely from indoor and outdoor air pollution (Im et al. 2015). Traffic and urbanization at local and regional levels affect air quality and ecosystems. In

✉ Abhishek Chakraborty
abhishekc@iitb.ac.in

¹ Environmental Science and Engineering Department, Indian Institute of Technology Bombay, Maharashtra 400076 Mumbai, India

Mumbai, the emission from the traffic sector nearly doubled in the past four years, from 16% (2016) to 30.5% (2019–2020) (SAFAR 2022). The risk of cardiopulmonary death is connected with long-term exposure, while respiratory difficulties are associated with short-term exposure (WHO 2013). The atmospheric particulate matter, one of the major air pollutants, impacts human health, visibility, and climate change (Kroll and Seinfeld 2008). The metals are a significant component of atmospheric particulate matters and cause various toxic effects and health risks. These metals bioaccumulate and interfere with the physiological functioning of the human body (Bolognini et al. 2009). They are the primary cause of oxidative stress in the body and mitochondrial damage, leading to cardiovascular mortality and morbidity (Araujo and Andre 2009).

Inorganic and organic components are present in particulate matter or atmospheric particulate matters. Organic aerosols (OA) make up a significant part of fine aerosol (Chakraborty et al. 2017). Oxidation, fragmentation, gas-to-particle conversion, precursor sources, and meteorology affect OA chemical composition. Also, it varies spatially and temporarily (Zhang et al. 2011). Organic and elemental carbon concentrations (OC & EC) are initially determined to measure organic particulate matter in PM (Turpin 1995). Visibility is significantly reduced by the EC, while solar radiation is scattered by the OC (Kirkevåg et al. 2013). In addition to reducing atmospheric visibility, this can alter the characteristics of clouds and precipitation radiation that affect global climate change (Jacobson 2016). A long-term, high-resolution dataset is required to understand EC-OC dynamics, determine their causes, and implement effective mitigation methods. As a result of incomplete combustion, EC is the most common product. On the other hand, anthropogenic or biogenic OC can be released directly into the atmosphere (primary organic carbon, POC), or oxidative species interact with organic precursors to produce less volatile products, which are then partitioned from gas to particle phase (secondary organic carbon, SOC) (Kroll 2008). OC consists of hundreds of molecules with different chemical and physical properties. It is difficult to directly estimate the contributions of primary and secondary organic particulate matter components by chemical analysis. A thermal optical analyzer (TOA) analyses the concentration of OC and EC based on the volatility of different organic and elemental carbon fractions in PM_{2.5} (Aslam et al. 2020).

According to IQAir, India was placed 5th place in 2021 on the most polluted country's list (IQAir 2022). The Indo-Gangetic Plain is the most polluted and studied region in India, and during winter, air quality is generally in the unhealthy to hazardous range. Compared to IGP, fewer studies were conducted in other parts of the country (Chowdhury et al. 2007; Joseph et al. 2012). The air quality in these cities falls under the unhealthy category (Aqi.in 2022), and one of them is Mumbai, the financial capital of India, which lies in the western part of India. The particulate matter concentration (PM) was nine times higher than the WHO limit in 2021 in Mumbai (IQAir 2022). The reported average PM_{2.5} for Mumbai in winter 2021 was 80 µg/m³ (SmartAIR 2022), above the NAAQ annual standard (40 µg/m³).

This study aims to examine the air quality of the metropolitan coastal city of India and the influence of air pollutants on the health of the residents. The spatial distribution of PM_{2.5} were studied for EC, OC and metal concentrations. The focus is on residential, low-density traffic, and high-density traffic sites. The particulate matter samples were collected during the day at all three locations. The impact of traffic on particulate matter concentration and composition is investigated. This study will help to investigate the effects of air pollutants on climate and human health and implement strategies for air pollution mitigation, particularly in heavy traffic-impacted megacities such as Mumbai.

2 Research methodology

2.1 Sampling sites and sample collection

The organic carbon concentration all over India is in a higher range, even in western India (Fig. 1). In this study, November and December were covered for sampling. Measurements were performed in Mumbai, at the Indian Institute of Technology Bombay (IITB) campus, and Sakinaka, a traffic Junction (Fig. 1).

In IITB, two locations were chosen, one is close to the road (YP-Gate), and another is a residential site (Hostel Premise, HP). The sampling location at YP-Gate has modest traffic, whereas Sakinaka has significantly higher traffic volumes than YP gate (www.tomtom.com; [Deadliest traffic Junction](#)). The $PM_{2.5}$ samples were taken using a mini volume sampler for 10 h (9:00AM to 7:00PM) at a flow rate of 5 L per min on 47 mm quartz microfiber and Teflon (PTFE) filters. Quartz filters were heated at 600 °C for 6 h in a muffle furnace to remove organic impurities before sampling. The sampling was performed on alternate days from November to December (2021) and total 23 (15 Quartz and 8 Teflon) filters were collected at each YP-Gate and Hostel premise, whereas 16 (8 Quartz and 8 Teflon) filters were collected at Sakinaka Junction simultaneously. An optical Particle Counter (OPC) was used to capture PM size and mass distribution at each location, and sampling was done simultaneously with a mini vol sampler (Tomtom traffic index 2021).

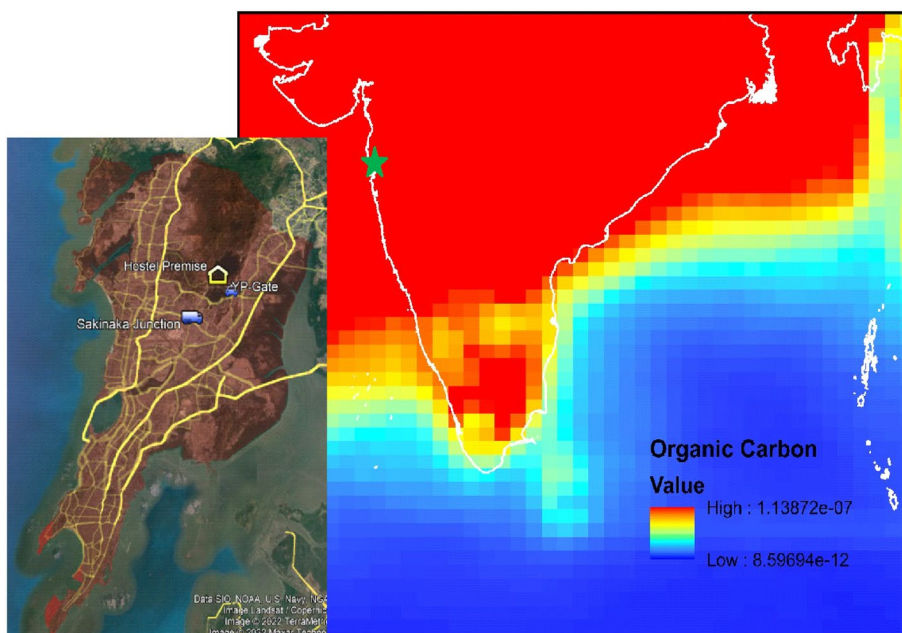


Fig. 1 Study location according to emissions sources, Hostel Premise, YP-Gate, and Sakinaka-Junction in Mumbai (Merra reanalysis data 2022). (Source: Google Earth Pro and MERRA reanalysis data Giovanni and unit of organic carbon is kg/m^3)

2.2 Measurement and analysis of PM_{2.5} samples

The TOA from DRI was used to measure OC and EC concentrations in PM_{2.5} samples collected on quartz filters. The methodology used for analysis is based on IMPROVE (Birch 1998). The sampling analysis is divided into two phases. As a first step, OC is volatilized from the sample in a non-oxidizing environment at different temperatures (340 °C, 500 °C, and 615 °C) for 60 and 90 s (870 °C). Second, the oven is cooled to below 500 °C for 60 s, and helium and oxygen are introduced. The temperature gradually increases to 850 °C, maintained for 45 s, and 900 °C for 120 s. Four OC fractions, pyrolyzed carbon, and three EC fractions were produced on the thermograph (Jamhari et al. 2022). PM's elemental components (Si, Ti, Mn, Zn, As, and Se) were analyzed using Teflon filters by energy-dispersive X-ray fluorescence (EDXRF). A spiked quantity of element mass was used to determine element recovery efficiencies. The inorganic components of PM are analyzed by using the ion chromatography method. The samples collected on quartz filters were extracted ultrasonically for 120 min using 20 ml of deionized water. The insoluble matters were filtered out by using 0.22 µm nylon membrane filters then the sample was analyzed in an ion chromatography system for the concentration of each cation (Na⁺, K⁺, NH₄⁺, Ca²⁺) and anion (Cl⁻, F⁻, Br⁻, NO₃⁻, SO₄²⁻). The blank filters were also analyzed for blank corrections. The peak was observed against a standard solution.

The standards were prepared and analysed in IC at the beginning of the analysis and after every 10 analytical runs. The obtained values were analysed and compared with values obtained during previous quality control tests, if the difference is less than 10% then only we proceed with the sample analysis. A correlation graph was plotted between the known value of the standard and the obtained value (IC) for quality assurance (QA), and filter samples were only analysed if the correlation exceeded 0.995. The detection limit for IC was the three times the standard deviation in lab blank filters.

2.3 Exposure assessment

Air pollution in these areas is likely to expose residents to metals. They are classified based on age group, children (0–15) and adults (Sah et al. 2019). The risk of heavy metals in PM_{2.5} is assessed based on daily chemical intake (CDI), dermal absorbed dose (DAD), and exposure concentration (EC) is calculated according to the human health evaluation manual (Part A), as well as additional guidance for assessing dermal risk (Part E) and inhalation Part F. The following were the equations and abbreviations mentioned in the supplementary document (Table SI 1):

$$CDI(ingest) = [(C \times IngR)/BW] \times [(EF \times ED)/AT] \times CF \quad (1)$$

$$DAD(dermal) = [(C \times SA \times AF \times ABS)/BW] \times [(EF \times ED)/AT] \times CF \quad (2)$$

$$EC(Inhalation) = (C \times ET \times EF \times ED)/AT_n \quad (3)$$

where: C is the metal concentrations, IngR: is ingestion rate; ED: is exposure duration; EF: is exposure frequency; BW: is body weight; AT: averaging time, CF: is the conversion factor, SA: is skin surface area exposed to airborne particulates; AF: adhesion factor for

airborne particles on the skin; ABS: absorption factor dermal; ET: exposure time; ATn: average time calculated by multiplying 24 by the AT.

Risks were quantified independently for non-carcinogenic and carcinogenic impacts. A hazard quotient was used to assess the non-carcinogenic danger (HQ) and cancer risk (CR) for carcinogenic effects. The following equations were used to evaluate the HQ and CR of heavy metals in PM_{2.5} via ingestion, dermal contact, and inhalation.

$$HQ = \frac{CDI}{RfDo} = \frac{DAD}{(RfDo \times GIABS)} = \frac{EC}{(RfCi \times 1000 \mu\text{gmg}^{-1})} \quad (4)$$

$$CR = CDI \times Sfo = DAD \times \left(\frac{Sfo}{GIABS} \right) = IUR \times EC \quad (5)$$

Sfo, RfDo, RfCi, GIABS, and IUR are taken from US environmental protection agency screening level report (USEPA 2011). The RfDo is oral reference dose, RfCi is inhalation reference concentration, Sfo is oral slope factor, GIABS is gastrointestinal absorption factor, and IUR is inhalation unit risk.

2.4 Human respiratory tract deposition model

The multiple path particle dosimetry models (MPPD, v3.04) calculate particulate matter's deposition fraction at different parts of the human lungs. This model can calculate regional and overall PM deposition and clearance from the other respiratory system parts. The input parameters of this model are (1) airway morphology, (2) particle properties, and (3) exposure scenarios. The detail of the model description can be found in various studies (Lv et al. 2021; Zwodziak et al. 2017). The human airway morphology differs for adults and children, so an age-specific 5-lobe model was used in this study (Menache 1995). The model was run for two scenarios, i.e., adults and children (Multiple-Path Particle Dosimetry Model (MPPD) 2022).

3 Result and discussion

3.1 Meteorological parameters

The climate of Mumbai is wet & dry tropical and highly influenced by the Asian monsoon. The distinction between summer and winter is not significant. During sampling time, the average planetary boundary layer height (PBLH) was 772 m during the day and 661 m at night (Merra data NASA). The average temperature was between 25 and 32 °C, and relative humidity was 40–50% (CPCB.nic.in, 2022). The wind rose for HP, and the YP-Gate site was obtained from the MPCB monitoring station (Powai), depicting that the wind had blown from YP-Gate to HP (Fig. SI 1). The nearest CPCB station for Sakinaka is 2 km from the sampling site, so it would not be a true representation of wind patterns at the Sakinaka site. With the Hybrid Single-Particle Lagrangian Integrated Trajectory model (HYSPPLIT, 2022), backward trajectories of air masses arriving at a specific location can be generated. This model indicates that in Mumbai city, air came from the inland area during the sampling (Fig. SI 2).

3.2 PM size and mass distribution

The PM_{10} , $PM_{2.5}$, and PM_1 concentrations at all three locations are mentioned in Table SI 2, along with some other global studies. The highest PM concentrations are reported at Sakinaka and the lowest at HP. PM deposited on the lung surface can induce tissue damage, corrode the alveolar wall, and impair the lung (Douglas et al. 2018; Xing et al. 2019). The $PM_1/PM_{2.5}$ and $PM_{2.5}/PM_{10}$ ratios are higher at HP (0.72 & 0.78), followed by YP (0.62 & 0.78) and Sakinaka (0.49 & 0.56), denoting the enhancement of fine mode particles in HP and YP. The lower ratio in Sakinaka suggests the dominance of coarse mode particles (Chauhan 2021). The coarse-size particle sources were road abrasion, brake, and tire wear (Kumar et al. 2018). Furthermore, commuters were more at the sampling location since the Sakinaka metro station was nearby, so coarse particles remained resuspended due to various movements.

The lognormal mass size distribution in the morning, fine PM mass distribution peak (9 AM to 11 AM) was highest compared to other times of the day at Sakinaka (Fig. 2). Also, the maximum peak was observed at 0.25 and 0.9 μm . The YP-Gate is close to the traffic site, so the particles were highest in the morning, whereas at HP (residential area), these were highest in the noon hours. The PM mass size distribution peak was observed at 0.4 μm in HP and 0.33 μm in YP-Gate. The normalized number concentration also shows that the same peak was observed around 0.4 μm in HP (Fig. SI 3). The distribution pattern and particulate matter peak at Sakinaka differed from the other two locations.

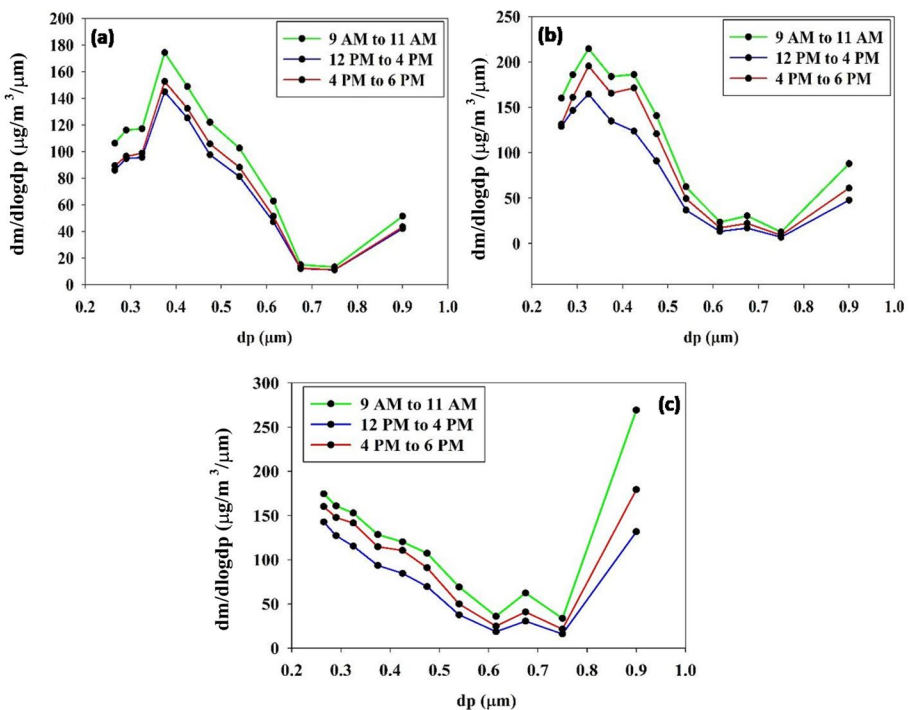


Fig. 2 Lognormal mass size distribution of fine particulate matter at different locations **a** HP, **b** YP-Gate, and **c** Sakinaka

3.3 Carbonaceous particulate matter distribution and levels

Mean EC levels were $3.5 \mu\text{g}/\text{m}^3$, $8.5 \mu\text{g}/\text{m}^3$, and $13 \mu\text{g}/\text{m}^3$ for HP, YP-Gate, and Sakinaka sites, respectively (Fig. 3a). The OC concentration was $15.5 \mu\text{g}/\text{m}^3$, $22 \mu\text{g}/\text{m}^3$, and $35 \mu\text{g}/\text{m}^3$ respectively (Fig. 3b). Among these three sites, average OC and EC concentrations were highest at Sakinaka, attributable to the mixed contribution from high traffic flows. Due to its downwind location (Fig. SI 1) from anthropogenic emission sources, HP had the lowest concentrations of OC and EC. The study conducted in the year 2007 reported OC concentrations were $28 \mu\text{g}/\text{m}^3$ and $31 \mu\text{g}/\text{m}^3$, whereas EC concentrations were $9 \mu\text{g}/\text{m}^3$ and $7 \mu\text{g}/\text{m}^3$ (Joseph et al. 2012). Compared to previous studies, this study's OC & EC concentration is comparable and even slightly higher. The average values for the OC/EC ratio were 4.5, 2.5, and 2.8 at HP, YP-Gate, and Sakinaka sites, respectively; OC/EC ratios greater than 2 have been considered an indicator of SOA formation due to contributions to OC from both combustion sources and secondary formation of carbonaceous materials (Hildemann et al. 1991). High OC by EC ratio in $\text{PM}_{2.5}$ denotes dominance of secondary organics fraction in fine particulate matter. PM composition in Sakinaka may be receiving more contributions from resuspended road dust due to higher traffic volumes.

The organic aerosol (OA) is calculated by multiplying OC by 2 (for an urban area), as many Indian studies indicated the same based on online and offline organic aerosol characterization (Chakraborty et al. 2017). Total carbonaceous aerosol (TCA) is estimated by the sum of EC and OA [$\text{TCA} = 2 \times \text{OC}$ (or OA) + EC] (Rengarajan et al. 2007; Turpin et al. 1995). The OA contribution to $\text{PM}_{2.5}$ (29.6%) is more at Sakinaka than at the other two sites. The EC values were also higher at Sakinaka due to primary vehicular emissions. The mean TCA concentrations were 34.5 , 52.5 , and $83 \mu\text{g}/\text{m}^3$ at HP, YP-Gate, and Sakinaka, respectively. Anthropogenic emissions of carbonaceous particulate matter and unfavorable meteorological conditions may contribute to the higher TCA contribution, such as low wind speed, low mixing height, frequent inversions, etc., resulting in pollution stagnation (Pachauri et al. 2013).

The chemical characterization of $\text{PM}_{2.5}$ samples at all three locations has shown that anions at HP have the highest percentage of $\text{PM}_{2.5}$ than the other two locations (Fig. 4). The percentage of cations and anions is higher in the coastal region $\text{PM}_{2.5}$ in comparison to the inland region (Table SI 3). The transportation sector is the major source of nitrate and residential activities for sulfate (Zhang et al. 2012). The higher fractions of Na and Cl in all the sites might indicate sea salts.

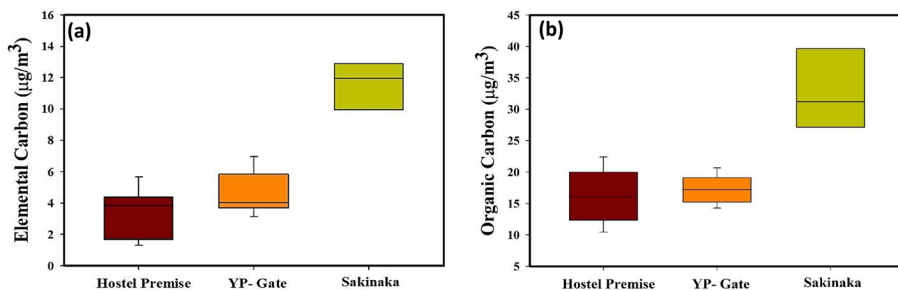


Fig. 3 Average concentration of the **a** Elemental carbon and **b** Organic carbon at the study locations, HP, YP-Gate, and Sakinaka

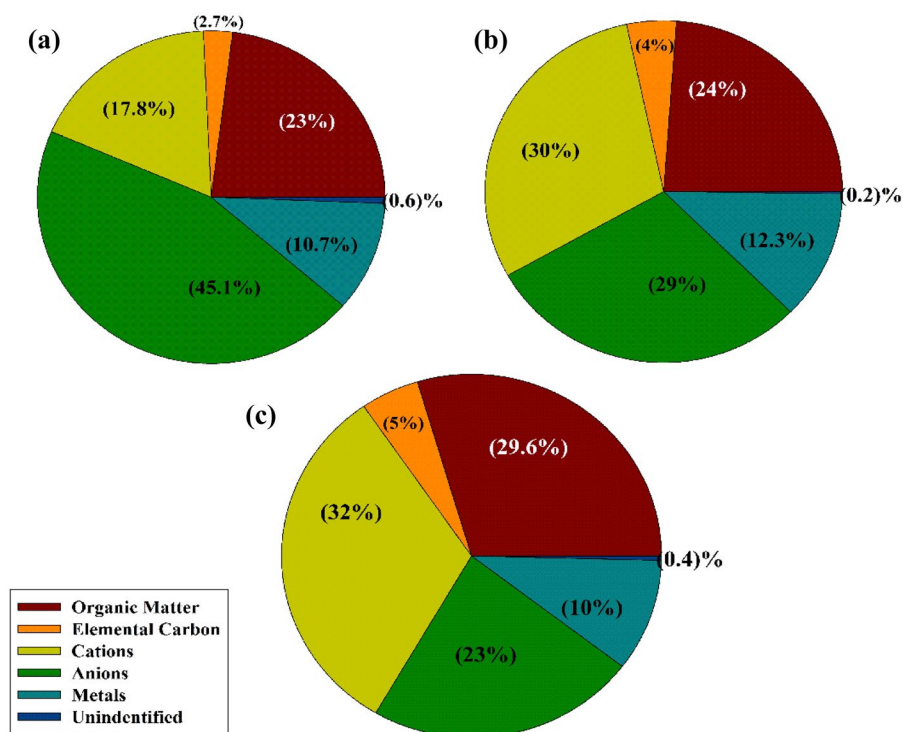


Fig. 4 The $PM_{2.5}$ chemical characterization at different locations in Mumbai, **a** HP, **b** YP-Gate and, **c** Sakinaka Junction

3.4 The volatility of organic aerosol

The OC fraction is analyzed by a TOA (Section 2.2) based on its volatility. Four temperature-resolved OC fractions (OC1, OC2, OC3, and OC4) are obtained, with OC1 to OC4 having decreasing volatility. This atmospheric OC property (volatility) has been utilized to distinguish between distinct sources of PM, total OC, and OC volatility fractions in various metropolitan settings (Soleimani et al. 2019). The OC1 exists mostly in the vapor phase (Liu et al. 2006). The OC2 and OC3 fractions in the particulate matter come from the gasoline and diesel factor (Kim and Hopke 2004). The PMF study showed that OC4 is mainly associated with secondary coal sources that have traveled farther from local traffic emitted OC (Lee et al. 2003). The OC and EC levels vary at all three locations (Table SI 4). The concentration of OC1 is nil in all three areas, and the other fractions of OCs (OC2 to OC4) were highest at Sakinaka compared to YP-Gate and HP. OC2 and OC3 concentrations at Sakinaka were way higher than OC4 concentrations. Sakinaka is a traffic site with very high and continuous traffic volumes, so OC2 and OC3 values were higher in Sakinaka. Though YP-Gate is also close to the traffic location, the concentration of OC2 and OC3 was less than in Sakinaka. The OC4 concentration at the HP was slightly higher than YP-Gate. Contribution of low volatile organic fraction (OC4) fraction to total OC was 0.21, 0.16, and 0.19 at HP, YP-Gate, and Sakinaka, respectively. The higher volatile OC fraction (OC2 and OC3) in total OC was 0.66, 0.56, and 0.79 at the HP, YP-Gate, and Sakinaka. The HP had a higher

fraction of low volatile OC than the other two traffic sites, indicating more dominance of secondary organics. In contrast, Sakinaka has a more high-volatile OC fraction in total OC, indicating more primary organics emissions during sampling. YP-Gate's mean OC value is between the Sakinaka and HP's values in both scenarios denoting a mixture of traffic emissions and secondary formation.

3.5 Char-EC and soot-EC

Emissions of EC come mainly from combustion emissions, which are primarily anthropogenic (tire exhaust and fossil fuel and biomass combustion) and divided into char and soot. Char and soot are separated by size and range from heavily condensed refractory submicron soot particles to large pieces of lightly charred material (Han et al. 2007; Zhan et al. 2019). Char-EC/Soot-EC ratios have been used to identify sources (Han et al. 2009). Char is produced by burning solid residues, whereas soot is produced by incomplete combustion. Depending on the type of combustion, their ratios will vary between different source categories (Han et al. 2010). Char-EC is the difference between EC1 and OP, and soot-EC is the sum of EC2 and EC3. Residential cooking produces char-EC/soot-EC, generally within the range of 2.0 to 6.0 (Chow et al. 2004). Higher char/soot ratios indicate the major influence of biomass combustion and coal combustion, whereas lower char/soot ratios indicate the major impact of vehicular exhaust (Wang et al. 2019). The spatial distribution of the ratio is shown in Table SI 5. Additionally, the relationship between OC and EC can be used to assess the origin of carbonaceous particulate matter (Cao et al. 2006). OC/EC for biomass combustion was 6.6, and 0.7 for motor vehicle emissions (Saarikoski et al. 2008). A ratio of OC/EC above 5 can indicate increased biomass burning, while OC/EC ratios below 2 may indicate fossil fuel combustion or motor vehicle emissions (Rastogi et al. 2016). As discussed in Section 3.3, OC/EC ratios range from 2.8 to 4.5, indicating diverse emissions sources from biomass burning and vehicular emissions (Table SI 5).

Char-EC and Soot-EC have the highest correlation at Sakinaka, with an R^2 value of 0.8 ($p < 0.05$) (Fig. SI 4). Char-EC and Soot-EC are likely to originate from fuel combustion in vehicular engines. On the other hand, YP-Gate and HP have positive but relatively lower R^2 values, around 0.6. This indicates different sources and formation mechanisms, such as char formed from combustion residues and soot formed by gas conversion (Zhan et al. 2019).

3.6 Metal concentration and emission factor

High airborne trace element concentrations can negatively impact air quality and human health (Xia 2011). As metals derived from pollution are frequently concentrated on small particles, they may stay suspended in the air for extended periods and effectively enter the human lungs. Therefore, the particulate toxicity of fine aerosol particles may be influenced by trace metals (Gao et al. 2002). The crustal-originated metal concentrations, i.e., Al, Ca, and Fe, are higher in HP. In contrast, industrial and traffic-related metals are more elevated in YP-Gate and Sakinaka, i.e., Ba, Cu, Cr, Mn, Pb, Zn, and As (Table SI 6). After oxygen and silicon, Al and Fe are the third and fourth most abundant metals in the Earth's crust, with a typical Fe/Al ratio of approximately 0.44 for the upper continental crust (Rudnick 2000). In this study, the ratios are 1.08, 1.48, and 1.56 at HP, YP-Gate, and Sakinaka, respectively, which is more than the crustal ratio and indicates anthropogenic contamination of the dust at these locations. Near the traffic junction, the highest ratio indicates some traffic originated Fe. The ratio of Fe/Al in soil

resuspension is around ~ 0.9 (Engelbrecht et al. 2016), close to the ratio obtained for HP. Cu concentrations in all three locations were low, so the ratios of Cu/Zn and Cu/Pb are also low compared to road dust (0.17 and 0.96, respectively) (Shen et al. 2016) (Fig. 5). The Ca/Al, and Mg/Al ratios are higher than the crustal ratio, i.e., 0.37 and 0.17, respectively (Mclennan 2001). The K/Al ratio was significantly higher than upper continental crustal values (0.35) at HP (4.9), followed by YP (4.5) and Sakinaka (1.7). Potassium is generally an indicator of biomass burning emissions.

The enrichment factor (EF) is calculated to study the impact of anthropogenic emissions on these metals in $PM_{2.5}$. The EF is also widely used for the source identification of chemical constituents of $PM_{2.5}$ samples. It is calculated by comparing elements' concentration in the ambient aerosol to their concentration present in the Earth's crust. The element's crustal concentration has been taken from Hans Wedepohl 1995. The EF is calculated using Eq. (3) by taking aluminum (Al) as a reference element for a geogenic source (Mehra et al. 2020).

All the value of EF above 10 is plotted in Fig. 6. The degree of Lead enrichment (Pb) is high in all the locations, i.e., 1707.63 (Sakinaka), 1676.78 (YP-Gate), and 391.93 (HP), and for Arsenic (As) is 3100, 3593.8 and 8490 respectively. Zinc (Zn), Copper (Cu), and Bromine (Br) have high EF values, in between the range of 10–1000. The sulfur enrichment is varied in Sakinaka > YP-Gate > HP decreasing manner. Cu is also a tracer of traffic emissions (Dongarrà et al. 2007). Sources of sulfur are fossil fuel and biomass-burning emissions (Reddy and Venkataraman 2002). Even though the EF values of metals are higher at YP and Sakinaka, the percentage of metal concentration in total $PM_{2.5}$ is slightly higher in HP samples. The crustal metals contribute more to $PM_{2.5}$ than the anthropogenic ones at HP, whereas traffic sites have more anthropogenically emitted metals in $PM_{2.5}$. EF value for Cd is reported in the range of 1000–15,000 in various studies at urban sites (Jack et al. 2020; Li et al. 2016; Lin and Wang 2020). The toxic heavy metals are more enriched in traffic samples, i.e., As, Cd, and Pb. High enrichment of these metals suggests the dominant source is anthropogenic activities, like traffic emissions and biomass burning. Long-term exposure to arsenic and Cd can cause cancer of the bladder and lungs, whereas lead exposure could cause kidney and brain damage (WHO 2018 and NIOSH).

Fig. 5 Elemental ratios at different sites (Left axis for Cu/Pb and Cu/Zn ratio)

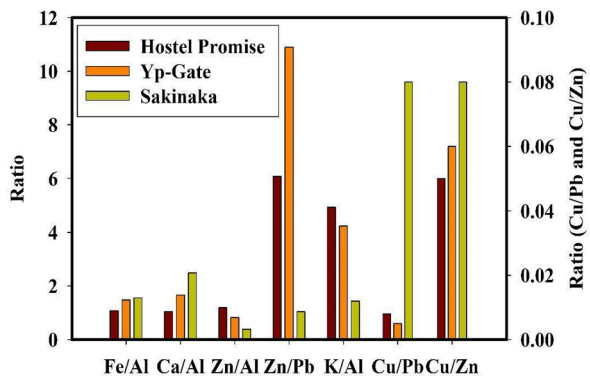
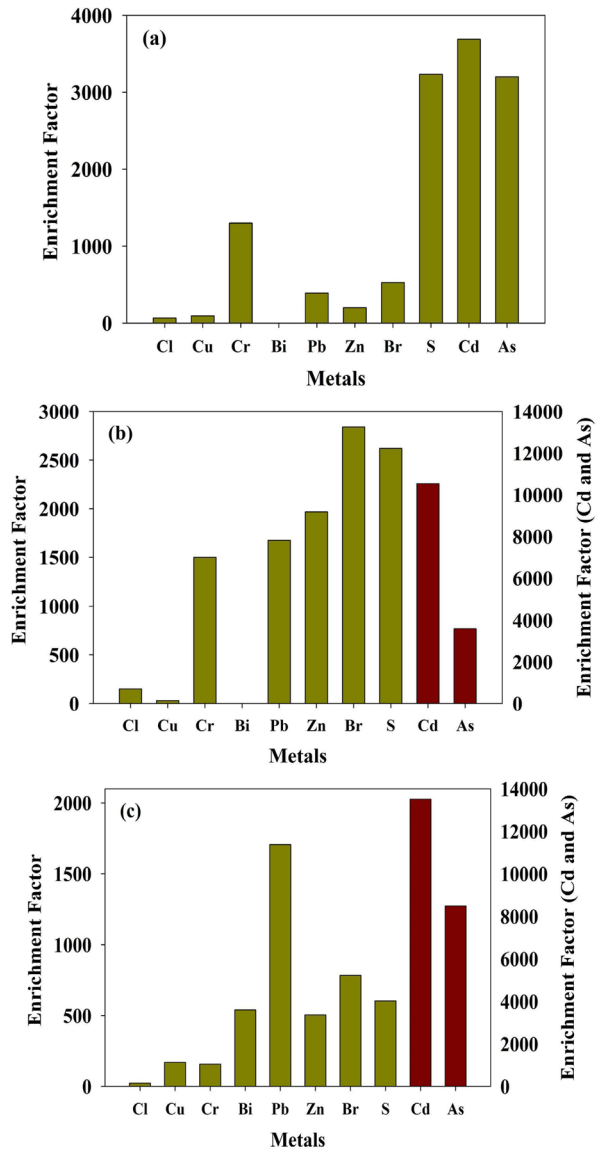


Fig. 6 Enrichment factor of metals in PM_{2.5} at **a** HP, **b** YP-Gate, and **c** Sakinaka (For YP-Gate and Sakinaka, two scales are used for high value)



3.7 Exposure assessment of heavy metals and lung deposition

Daily exposure to air pollutants has serious health problems. Some metals in the particulate matter have carcinogenic risk (CR) that increases the toxicity of particulate matter. The acceptable limit for total CR is from 1×10^{-6} to 1×10^{-4} . The non-carcinogenic metals are still hazardous to human health and are assessed under Hazard Quotient (HQ). The Hazard Index (HI) is the sum of HQ of all the non-carcinogenic metals (Sui et al. 2020). If the HI is below 1, it does not possess any harmful effects but has serious health issues if it is above 1. The hazardous and toxic metals are studied in this study for their carcinogenic and

non-carcinogenic effects on Adults' and Children's health. The hazard risk and cancer risk for inhalation, digestion, and dermal exposure are calculated (Section 2.3), and the result is summarised in Tables 1 and SI 7 and 8.

The HI value for children's exposure assessment for inhalation is greater than 1 at all locations. The CR value for inhalation is higher than 1×10^{-4} at all three locations. Sakinaka is a congested area in terms of traffic and various shops (DriveU Blog). The nearest metro station to the sampling site also adds extra crowding during office morning/evening hours. Due to this situation, health is more at risk from exposure. Cd, As, and Cr metals are the main contributors to CR and HI. The toxicity effect of metals through dermal and ingestion is under the safe limit at all three locations (Table SI 7 and 8). These findings indicate elemental exposure from dermal and ingestion will not result in non-carcinogenic and carcinogenic adverse effects on adults and children. Whereas through inhalation, $PM_{2.5}$ causes health risks in both adults and children.

The MPPD model is used to estimate PM deposition through inhalation. The count median diameter and the geometric standard deviation are required in this model, along with PM concentration as model input (Manojkumar and Srimuruganandam 2022). The calculated deposited mass (μg) of PM in the lung is represented in Fig. SI 5 for adults (Age 21) and children (Age 14). The mass deposition in adults is higher than in children. The highest deposition is observed in residents of the Sakinaka site, followed by YP-Gate and HP. Sakinaka residents are more prone to health risks from PM than the other two sites. Among all study sites, depositions of $PM_{2.5}$ were highest in the head region (42%), whereas PM_1 depositions were highest in the pulmonary (59%). Ultrafine particles should be included in the current air-quality index since they are most prevalent in the lungs.

Table 1 Hazard and cancer risk index for inhalation at all three locations for adults and Children

Hazard Index for inhalation						
Metals	Sakinaka		YP-Gate		HP	
	HQ (Adult)	HQ (Children)	HQ (Adult)	HQ (Children)	HQ (Adult)	HQ (Children)
Cr	2.3	2.3	0.033	0.033	0.03	0.03
Mn	0.16	0.16	0.21	0.21	0.2	0.2
Pb	0.38	0.38	0.14	0.14	0.06	0.06
S	2.1	2.1	3.2	3.2	3	3
Ti	0.3	0.3	0.13	0.13	0.06	0.06
Cd	4.9	4.9	0.16	0.16	0.43	0.43
As	0.5	0.5	0.82	0.82	0.6	0.6
HI	11	11	4.7	4.7	4.4	4.4
Cancer Risk for inhalation						
Metals	Sakinaka		YP-Gate		HP	
	CR (Adult)	CR (Children)	CR (Adult)	CR (Children)	CR (Adult)	CR (Children)
Cr	6.6E-07	1.7E-07	9.5E-05	2.4E-05	9.0E-05	2.2E-05
Pb	5.1E-07	1.3E-07	1.9E-03	4.6E-04	8.5E-04	2.1E-04
Cd	3.0E-06	7.6E-07	1.0E-06	2.5E-07	2.6E-06	6.6E-07
As	7.3E-05	1.8E-05	1.2E-05	3.6E-06	9.7E-06	2.4E-06
Total CR	1.2E-02	2.9E-03	2.0E-03	4.9E-04	8.9E-04	2.3E-04

4 Conclusions

EC concentrations were highest at Sakinaka and lowest at HP due to its location upwind of anthropogenic emission sources (YP-Gate). On the other hand, the OC/EC ratio was highest at HP due to contributions to OC from stationary combustion sources and secondary production processes. The TCA percentage in $PM_{2.5}$ ranges from 33 to 55%, demonstrating that carbonaceous species are abundant in fine particles at all three sampling sites. The OC fractions are also differentiated based on volatility, and the HP has a high percentage of low-volatile OC fractions, while Sakinaka has high-volatile OC fractions. The ratio of OC/EC and percentage of OC fractions in total OC show the diverse nature of $PM_{2.5}$ samples. Sakinaka is traffic influenced, and the HP is a residential site, but YP-Gate is low-density traffic with a residential area. Char-EC and Soot-EC ratios indicate the same; the HP ratio implies biomass-burning sources, while Sakinaka and YP-Gate suggest vehicular emissions and biofuel burning.

The organic and inorganic compounds were high in Sakinaka samples because of the high emissions at this site. YP-Gate has lower emissions than Sakinaka, followed by HP. The crustal-originated metal concentrations, i.e., Al, Ca, and Fe, are higher in HP. In contrast, industrial and traffic-related metals are higher in YP-Gate and Sakinaka, i.e., Ba, Cu, Cr, Mn, Pb, Zn, and As. The ratio of these metals also suggested anthropogenic source contribution to the particulate matter, i.e., traffic and biomass burning emissions. The enrichment factor of these metals is way higher in Sakinaka samples compared to HP and YP-Gate. The assessment of the cancer risk from these heavy metals has shown a risk of cancer in adults and children of all these three locations' residents through chronic daily intake via inhalation of pollutants in their lifetime. The lung deposition model also showed that PM deposition is higher in residents of Sakinaka. So, in conclusion, Sakinaka is at higher risk for the health effects of emissions of air pollutants. YP-Gate has also shown the impact of traffic emissions on air quality and influences the HP pollutants concentration. The findings of this study clearly show that even in a coastal city like Mumbai, air quality issues are severe, and the exposed population is at risk of developing health issues. Given the tremendous heterogeneity observed in PM levels and composition at different locations, policymakers should develop area-specific pollution mitigation measures to improve the city's air quality.

Supplementary Information The online version contains supplementary material available at <https://doi.org/10.1007/s10874-023-09448-5>.

Author contributions Shruti Tripathi-Conceptualization; Data curation; Formal analysis; Methodology; and Writing original draft. Abhishek Chakraborty- Supervision, reviewed and edited. Debayan Mandal- Review and editing.

Funding The authors declare that no funds, grants, or other support were received during the preparation of this manuscript.

Data availability The datasets generated during and analyzed during the current study are not publicly available but are available from the corresponding author at a reasonable request.

Declarations

Competing interests The authors declare no competing interests.

Ethics approval Not applicable.

Consent to participate Not applicable.

Consent to publish Not applicable.

References

- 5-deadliest traffic junctions in Mumbai. <https://blog.driveu.in/5-deadliest-traffic-junctions-in-mumbai-85e66c4b0b3b>. Accessed 01 Oct 2021
- Air resource laboratory-Hysplit. <https://www.ready.noaa.gov/HYSPLIT.php> (2022). Accessed 18 Jul 2022
- AQI. <https://www.aqi.in/world-most-polluted-cities> (2022). Accessed 10 Apr 2022
- Araujo, J.A., Andre, E.N.: Particle and Fibre Toxicology Particulate Matter and atherosclerosis: Role of particle size, composition and oxidative stress. (2009). <http://www.particleandfibretoxicology.com/content/6/1/24>
- Aslam, A., et al.: Pollution characteristics of Particulate Matter (PM_{2.5} and PM₁₀) and Constituent Carbonaceous Aerosols in a south Asian future megacity. *Appl. Sci.* (Switzerland) **10**(24), 1–17 (2020)
- Birch, M., Eileen: Analysis of Carbonaceous Aerosols: Interlaboratory comparison. *Analyst* **123**(5), 851–857 (1998)
- Bolognin, S., et al.: Metal Ion Physiopathology in Neurodegenerative Disorders. (2009)
- Cao, J.J., et al.: Characterization of Roadside Fine Particulate Carbon and its eight fractions in Hong Kong. *Aerosol Air Qual. Res.* **6**(2), 106–122 (2006)
- Central Pollution Control Board. <https://www.cpcb.nic.in> (2022). Accessed 20 Apr 2022
- Chakraborty, A., Tripathi, S.N., Gupta, T.: Effects of Organic Aerosol Loading and Fog Processing on Organic Aerosol Volatility. *J. Aerosol Sci.* **105**(November 2016), 73–83 (2017). <https://doi.org/10.1016/j.jaerosci.2016.11.015>
- Chauhan, A.: Effect of lockdown on HCHO and trace gases over India during March 2020. *Aerosol Air Qual. Res.* **21**(4), 1–19 (2021)
- Chow, J.C., et al.: Source profiles for industrial, mobile, and area sources in the Big Bend Regional Aerosol visibility and observational study. *Chemosphere* **54**(2), 185–208 (2004)
- Chowdhury, Z., et al.: Speciation of ambient fine Organic Carbon particles and source apportionment of PM_{2.5} in indian cities. *J. Geophys. Res. Atmos* **112**(15), 1–14 (2007)
- Dongarrà, G., Manno, E., Varrica, D., Vultaggio, M.: Mass levels, crustal component and trace elements in PM₁₀ in Palermo, Italy. *Atmos. Environ* **41**(36), 7977–7986 (2007)
- Douglas, P., et al.: A systematic review of the Public Health Risks of Bioaerosols from Intensive Farming. *Int. J. Hyg. Environ Health* **221**(2), 134–173 (2018)
- Engelbrecht, J.P., et al.: Technical note: Mineralogical, chemical, morphological, and optical interrelationships of mineral dust resuspensions. *Atmos. Chem. Phys* **16**(17), 10809–10830 (2016). (14 Sept 2022)
- Gao, Y., et al.: Characterization of Atmospheric Trace Elements on PM_{2.5} particulate matter over the New York–New Jersey Harbor Estuary. *Atmos. Environ.* **36**(6), 1077–1086 (2002)
- Han, Y., et al.: Evaluation of the Thermal/Optical Reflectance Method for discrimination between Char- and Soot-EC. *Chemosphere* **69**(4), 569–574 (2007)
- Han, Y.M., et al.: Elemental Carbon in Urban Soils and Road Dusts in Xi'an, China and its implication for Air Pollution. *Atmos. Environ.* **43**(15), 2464–2470 (2009)
- Han, Y.M., et al.: Different characteristics of char and soot in the atmosphere and their ratio as an indicator for source identification in Xi'an, China. *Atmos. Chem. Phys.* **10**(2), 595–607. (2010). <https://acp.copernicus.org/articles/10/595/2010/> (14 Sep 2022)
- Hans Wedepohl, K.: The composition of the Continental Crust. *Geochim. Cosmochim. Acta* **59**(7), 1217–1232 (1995)
- Hildemann, L.M., Gregory, R., Markowski, Glen, R.C.: 25 In Onondaga County Monitoring Program Annual Report Heavy Metal Distribution in Particles from the Flocculent Sediments of Onondaga Lake. Wiley and Sons. (1991). <https://pubs.acs.org/sharingguidelines>
- Im, U., et al.: Evaluation of operational online-coupled Regional Air Quality Models over Europe and North America in the context of AQMEII phase 2. Part II: Particulate matter. *Atmos. Environ.* **115**, 421–441 (2015)
- IQAir. <https://www.iqair.com/in-en/>. Accessed 10 Apr 2022
- Jack, S.S., et al.: Pollution characteristics and chronic health risk assessment of metals and metalloids in ambient PM 2.5 in Licheng District, Jinan, China. *Environ. Geochem. Health* **42** (2020). <https://doi.org/10.1007/s10653-019-00448-7>
- Jacobson, M.Z.: Strong radiative heating due to mixing state of black carbon in atmospheric aerosol. *Mixing State of Black Carbon in Atmospheric Aerosols.* **409**(January 2001), 695–97 (2016)

- Jamhari, A.A., et al.: Seasonal variation and size distribution of Inorganic and Carbonaceous Components, source identification of size-fractioned Urban Air particles in Kuala Lumpur, Malaysia. *Chemosphere* **287**, 132309 (2022)
- Joseph, A., Elizabeth, S., Unnikrishnan: Chemical characterization and Mass Closure of Fine Aerosol for different land use patterns in Mumbai City. *Aerosol Air Qual. Res.* **12**(1), 61–72 (2012)
- Kim, E., Hopke, P.K.: Improving source identification of Atlanta Aerosol using temperature resolved Carbon fractions in positive Matrix Factorization. *Atmos. Environ.* **38**(20), 3349–3362 (2004)
- Kirkevåg, A., et al.: Aerosol–climate interactions in the norwegian Earth System model – NorESM1-M. *Geosci. Model Dev.* **6**(1), 207–244 (2013). ((November 8, 2022))
- Kroll, J.H.: Chemistry of secondary Organic Aerosol: Formation and evolution of low-volatility Organics in the atmosphere. *Atmos. Environ.* **42**(16), 3593–3624 (2008)
- Kumar, S., Nath, S., Bhatti, M.S., Yadav, S.: Chemical characteristics of fine and coarse particles during Wintertime over two Urban Cities in North India. *Aerosol Air Qual. Res.* **18**(7), 1573–1590 (2018)
- Lee, P.K.H., Brook, J.R., Dabek-Zlotorzynska, E., Mabury, S.A.: Identification of the major sources contributing to PM_{2.5} observed in Toronto. *Environmen Sci Technol.* **37**(21), 4831–4840 (2003). <https://doi.org/10.1021/es026473i>
- Li, H., et al.: Chemical characterization and source apportionment of PM_{2.5} aerosols in a megacity of Southeast China. *Atmos. Res.* **181**, 288–299 (2016)
- Lin, Y., Wang, J.: Concentrations, Enrichment, and sources of Metals in PM 2.5 in Beijing during Winter. (2020). <https://doi.org/10.1007/s11869-019-00763-z>
- Liu, W., Wang, Y., Russell, A., Edgerton, E.S.: Enhanced source identification of southeast aerosols using temperature-resolved carbon fractions and gas phase components. *Atmos Environ.* **40**(SUPPL. 2), 445–466 (2006). <https://doi.org/10.1016/J.ATMOSENV.2005.11.079>
- Lv, H., et al.: Assessment of Pedestrian exposure and deposition of PM₁₀, PM_{2.5} and Ultrafine particles at an urban Roadside: A case study of Xi'an, China. *Atmos. Pollut. Res.* **12**(4), 112–121 (2021)
- Manojkumar, N., Srimuruganandam, B.: Age-specific and seasonal deposition of outdoor and indoor particulate matter in human respiratory tract. *Atmos Pollut Res.* **13**(2) (2022). <https://doi.org/10.1016/j.apr.2021.101298>
- McLennan, S.M.: Relationships between the Trace Element Composition of Sedimentary Rocks and Upper Continental Crust. (2001)
- Mehra, M., Zirzow, F., Ram, K.: Geochemistry of PM_{2.5} aerosols at an urban site, Varanasi, in the Eastern Indo-Gangetic Plain during Pre-Monsoon season. *Atmos. Res.* **234**, 104734 (2020)
- Menache, M.: Particle inhalability curves for humans and small Laboratory Animals. *Ann. Occup. Hyg.* **39**(3), 317–328 (1995)
- Merra reanalysis data. <https://gmao.gsfc.nasa.gov/reanalysis/MERRA-2> (2022). Accessed 15 Jun 2022
- Multiple-Path Particle Dosimetry Model (MPPD). <https://www.ara.com/mppd/> (2022). Accessed 20 Aug 2022
- Pachauri, T., et al.: Characteristics and sources of Carbonaceous Aerosols in PM_{2.5} during Wintertime in Agra, India. *Aerosol Air Qual. Res.* **13**(3), 977–991 (2013)
- Rastogi, N., Singh, A., Sarin, M.M., Singh, D.: Temporal variability of primary and secondary aerosols over Northern India: Impact of Biomass Burning Emissions. *Atmos. Environ.* **125**, 396–403 (2016). <https://doi.org/10.1016/j.atmosenv.2015.06.010>
- Reddy, M., Shekar: Inventory of Aerosol and Sulphur Dioxide Emissions from India. Part II—Biomass Combustion. *Atmos. Environ.* **36**(4), 699–712 (2002)
- Rengarajan, R., Sarin, M.M., Sudheer, A.K.: Carbonaceous and inorganic Species in Atmospheric Aerosols during Wintertime over Urban and High-Altitude Sites in North India. *J. Geophys. Res. Atmos.* **112**(21), 1–16 (2007)
- Rudnick, R.L.: Rutile-Bearing Refractory Eclogites: Missing link between continents and depleted Mantle. *Science* **287**(5451), 278–281 (2000)
- Saarikoski, S., et al.: Sources of organic carbon in fine particulate matter in Northern European urban air. *Atmos. Chem. Phys.* **8**(20), 6281–6295 (2008)
- Sah, D., Verma, P.K., Kandikonda, M.K.: Pollution characteristics, Human Health risk through multiple exposure pathways, and source apportionment of Heavy Metals in PM₁₀ at Indo-Gangetic Site. *Urban Clim.* **27**, 149–162 (2019)
- Shen, Z., et al.: Chemical Profiles of urban fugitive Dust PM_{2.5} samples in Northern Chinese Cities. *Sci. Total Environ.* **569–570**, 619–626 (2016)
- SmartAIR. <https://smartairfilters.com/en/blog/mumbai-air-quality-exceeds-8-times-who-limit-in-2021/> (2022). Accessed 10 Apr 2022
- Soleimanian, E., et al.: Spatial Trends and sources of PM_{2.5} Organic Carbon volatility fractions (OC_x) across the Los Angeles Basin. *Atmos. Environ.* **209**, 201–211 (2019)

- Sui, S., et al.: Pollution characteristics and Chronic Health Risk Assessment of Metals and Metalloids in ambient PM_{2.5} in Licheng District, Jinan, China. *Environ. Geochem. Health* **42**(7), 1803–1815 (2020). <https://doi.org/10.1007/s10653-019-00448-7>
- System of Air Quality and Weather Forecasting And Research (SAFAR). <http://safar.tropmet.res.in/> (2022). Accessed 30 May 2022
- Tomtom traffic index. <https://www.tomtom.com> (2021). Accessed 01 Nov 2021
- Turpin, B.J.: Identification of secondary Organic aerosol episodes and quantitation of primary and secondary Organic aerosol concentrations during SCAQS. *Atmos. Environ.* **29**(23), 3527–3544 (1995)
- USEPA. <https://www.epa.gov/expobox/exposure-factors-handbook-2011-edition> (2011). Accessed 15 Apr 2022.
- Wang, F., Feng, T., Guo, Z., Li, Y., Lin, T., Rose, N.L.: Sources and dry deposition of carbonaceous aerosols over the coastal East China Sea: Implications for anthropogenic pollutant pathways and deposition. *Environ. Pollut.* **245**, 771–779 (2019). <https://doi.org/10.1016/j.envpol.2018.11.059>
- WHO: WHO health report. <https://www.who.int/about/accountability/results/2018-2019> (2018). Accessed 16 Apr 2022
- WHO: WHO health report. <https://apps.who.int/iris/handle/10665/107332> (2013). Accessed 10 Apr 2022
- Xia, L.: Characterization of Trace Elements in PM_{2.5} Aerosols in the vicinity of highways in Northeast New Jersey in the U.S. East Coast. *Atmos. Pollut. Res.* **2**(1), 34–44 (2011). <https://doi.org/10.5094/APR.2011.005>
- Xing, W., et al.: Inhalation bioaccessibility of cd, Cu, Pb and Zn and Speciation of Pb in particulate matter fractions from areas with different pollution characteristics in Henan Province, China. *Ecotoxicol. Environ. Saf.* **175**, 192–200 (2019)
- Zhan, C., et al.: Characterization of carbonaceous fractions in PM_{2.5} and PM₁₀ over a typical Industrial City in Central China. *Environ. Sci. Pollut. Res.* **26**(17), 16855–16867 (2019)
- Zhang, H., et al.: Source apportionment of PM_{2.5} nitrate and sulfate in China using a source-oriented Chemical Transport Model. *Atmos. Environ.* **62**, 228–242 (2012)
- Zhang, Q., et al.: Understanding Atmospheric Organic Aerosols via factor analysis of Aerosol Mass Spectrometry: A review. *Anal. Bioanal. Chem.* **401**(10), 3045–3067 (2011)
- Zwozdziak, A., et al.: Implications of the Aerosol size distribution Modal structure of Trace and Major elements on human exposure, inhaled dose and relevance to the PM_{2.5} and PM₁₀ Metrics in a european Pollution Hotspot Urban Area. *J. Aerosol. Sci.* **103**, 38–52 (2017)

Publisher's Note Springer Nature remains neutral with regard to jurisdictional claims in published maps and institutional affiliations.

Springer Nature or its licensor (e.g. a society or other partner) holds exclusive rights to this article under a publishing agreement with the author(s) or other rightsholder(s); author self-archiving of the accepted manuscript version of this article is solely governed by the terms of such publishing agreement and applicable law.